FA4869-06-1-0071 (AOARD-06-4076)

Research Final Report

Polymer-Oxide Nanolayer/Al Composite Cathode for

Efficient Polymer Light-Emitting Diodes

07/01/2006 ~ 06/30/2007

Name of Principal Investigator: Tzung-Fang Guo

E-mail address: guotf@mail.ncku.edu.tw

Institution: Institute of Electro-Optical Science and Engineering, National Cheng Kung University

Mailing address: No. 1 University Road, Tainan 701, Taiwan

Phone: +886-6-2757575 ext. 65284

FAX: +886-6-2747995

Co-investigators (names and institutions): Ten-Chin Wen,

Department of Chemical Engineering, National Cheng Kung University, Tainan 701, Taiwan

Report Documentation Page

Public reporting burden for the collection of information is estimated to average 1 hour per response, including the time for reviewing instructions, searching existing data sources, gathering and maintaining the data needed, and completing and reviewing the collection of information. Send comments regarding this burden estimate or any other aspect of this collection of information, including suggestions for reducing this burden, to Washington Headquarters Services, Directorate for Information Operations and Reports, 1215 Jefferson Davis Highway, Suite 1204, Arlington VA 22202-4302. Respondents should be aware that notwithstanding any other provision of law, no person shall be subject to a penalty for failing to comply with a collection of information if it does not display a currently valid OMB control number.

1. REPORT DATE **05 SEP 2007**	2. REPORT TYPE **FInal**	3. DATES COVERED **01-07-2006 to 30-06-2007**

4. TITLE AND SUBTITLE **Polymer-Oxide Nanolayer/Al Composite Cathode for Efficient Polymer Light-Emitting Diodes**	5a. CONTRACT NUMBER **FA48690610071**
	5b. GRANT NUMBER
	5c. PROGRAM ELEMENT NUMBER
6. AUTHOR(S) **Tzung-Fang Guo**	5d. PROJECT NUMBER
	5e. TASK NUMBER
	5f. WORK UNIT NUMBER
7. PERFORMING ORGANIZATION NAME(S) AND ADDRESS(ES) **National Cheng Kung University,No. 1 Univeristy Road,Tainan 701,Taiwan,TW,701**	8. PERFORMING ORGANIZATION REPORT NUMBER **N/A**
9. SPONSORING/MONITORING AGENCY NAME(S) AND ADDRESS(ES) **AOARD, UNIT 45002, APO, AP, 96337-5002**	10. SPONSOR/MONITOR'S ACRONYM(S) **AOARD**
	11. SPONSOR/MONITOR'S REPORT NUMBER(S) **AOARD-064076**

12. DISTRIBUTION/AVAILABILITY STATEMENT
Approved for public release; distribution unlimited

13. SUPPLEMENTARY NOTES

14. ABSTRACT
This research investigates the function of the polymer-oxide material as the interfacial buffer layer for the fabrication of high performance organic/polymer light-emitting diodes (O/PLEDs). The author proposed to place a salt-free, polymer-oxide nanolayer at the interface between the light-emissive polymer layer with Al as the device cathode instead of using low work function metals, such as Ca or LiF/Al. The processes for preparing the interfacial nanolayer can be easily integrated with the manufacturing procedures for the fabrication of O/PLEDs. The interfacial reaction and the mechanisms of the polymer nanolayer on the enhanced device performance had been well studied. The markedly enhanced device performance is presumed to be the instant formation of a specific carbon-Al complex nanolayer at the cathode interface during the deposition of Al. As a future project, the author has proposed the investigation of the unique organic-oxide nanolayer as the interfacial buffer structure for the fabrication of organic electronic devices.

15. SUBJECT TERMS

16. SECURITY CLASSIFICATION OF:			17. LIMITATION OF ABSTRACT	18. NUMBER OF PAGES	19a. NAME OF RESPONSIBLE PERSON
a. REPORT **unclassified**	b. ABSTRACT **unclassified**	c. THIS PAGE **unclassified**	**Same as Report (SAR)**	**37**	

Contents

I. Abstract

This research investigates the function of the polymer-oxide material as the interfacial buffer layer for the fabrication of high performance organic/polymer light-emitting diodes (O/PLEDs). We propose to place a salt-free, polymer-oxide nanolayer at the interface between the light-emissive polymer layer with Al as the device cathode instead of using low work function metals, such as Ca or LiF/Al. The processes for preparing the interfacial nanolayer can be easily integrated with the manufacturing procedures for the fabrication of O/PLEDs. The interfacial reaction and the mechanisms of the polymer nanolayer on the enhanced device performance had been well studied.

II. Technical milestones

- The study of the interfacial properties at the contact interface between the polymer-oxide nanolayer with the Al cathode. Extensive studies will be made by varying the polymer nanolayer with different thickness, functional groups and the metal cathode with different work functions. X-ray photoelectron spectroscopy, Raman scattering, Fourier transform infrared spectroscopy, and atomic force microscopy will be used to characterize the unique organic-metal properties of the interfacial nanolayer. We will summarized the results and disclose the correlations between the interfacial reaction with the device performance.

- The study of the high-brightness top-emissive polymer light-emitting diodes utilizing polymer oxide/Al/Ag composite cathode. This part of work focuses on the fabrication of high brightness top-emissive polymer light-emitting diode using the hybrid semi-transparent cathode, capable of the efficient injection of electrons. The composite cathode comprises the polymer oxide/Al complex as the injection buffer layer covered by a thin Ag overlayer. The optical micro-cavity effect is presumed to significantly promote the EL emission in the direction along the surface normal, which contributes the effective extraction of EL emission from the polymer oxide/Al/Ag composite cathode.

- The study of the polymer oxide/Al composite cathode in small molecular organic light-emitting diodes. Although the process (vacuum thermal evaporation) to prepare the polymer-oxide buffer layer can be easily integrated with the current manufacturing procedures to fabricate high-performance PLEDs, the devices exhibited an almost Ohmic current-voltage (*I-V*) characteristic and very low electroluminescence when the polymer oxide/Al composite cathode was applied

in the fabrication of small molecular OLEDs. Presumably, the electrical shorting of the device was caused by the interaction of the polymer oxide/Al complex material with the tris-(8-hydroxyquinoline) aluminum (Alq_3) layer. The deposited Al metal punctured the Alq_3/ N,N′-bis-(1-naphthyl)-N,N′-diphenyl-1,1′-biphenyl-4-4′-diamine (NPB) layers and made contact with the indium-tin-oxide (ITO)/glass anode. Extensive studies will be made to understand the mechanism of the interfacial reaction and provide a solution preventing the electrical short of the devices.

III. Summary of Accomplishments

1. High-brightness top-emissive polymer light-emitting diodes utilizing organic oxide/Al/Ag composite cathode
Appl. Phys. Lett., **89**, 051103, (2006). **(AOARD-06-4076)**

- High brightness (over 30,000 cd/m^2) top-emissive polymer light-emitting diodes (PLEDs) was fabricated by using a hybrid organic oxide/Al cathode, capable of the efficient injection of electrons.
- The optical micro-cavity effect significantly promotes the EL emission in the direction along the surface normal.

2. Organic oxide/Al composite cathode in organic/polymer light-emitting diodes
Appl. Phys. Lett., **89**, 053507, (2006). **(AOARD-06-4076)** **(This paper has also been selected for the August 14, 2006 issue of Virtual Journal of Nanoscale Science & Technology.)**

- Using an organic oxide/Al composite cathode to fabricate the small molecular organic light-emitting diodes (OLEDs).
- Incorporating the rubrene/poly(ethylene glycol) dimethyl ether (PEGDE) buffer layers into the composite cathode structure markedly improves the performance of devices. The luminous efficiencies of Alq_3-based OLEDs biased at ~ 100 mA/cm^2 are 4.8 cd/A and 5.1 cd/A for rubrene(50 Å)/PEGDE(15 Å)/Al and rubrene(50 Å)/PEGDE(15 Å)/LiF(5 Å)/Al cathode devices, 1.3 cd/A and 3.8 cd/A for devices with Al and LiF(5 Å)/Al cathodes, respectively.

3. Effect of TiO₂ nanoparticles on polymer-based bulk heterojunction solar cells

Jpn. J. Appl. Phys., **45**, L1314 (2006). **(AOARD-06-4076)**

4. Influence of polymer gate dielectrics on n-channel conduction of pentacene-based organic field-effect transistors

J. Appl. Phys. 101, 124505 (2007). **(AOARD-06-4076)**

5. Polymer/gold nanoparticles light emitting diodes utilizing high work function metal cathodes

Jpn. J. Appl. Phys. 46, 3A, 932 (2007). **(AOARD-06-4076)**

IV. High-brightness top-emissive polymer light-emitting diodes utilizing organic oxide/Al/Ag composite cathode

Tzung-Fang Guo,[a] Fuh-Shun Yang, Zen-Jay Tsai, Guan-Weng Feng

Institute of Electro-Optical Science and Engineering,

Advanced Optoelectronic Technology Center

National Cheng Kung University

Tainan, Taiwan 701, Republic of China

Ten-Chin Wen, Sung-Nien Hsieh

Department of Chemical Engineering

National Cheng Kung University

Tainan, Taiwan 701, Republic of China

Chia-Tin Chung, Ching-In Wu

Chi Mei Optoelectronics Corporation

Tainan Science-Based Industrial Park

Taiwan, 741, Republic of China

Abstract

This work presents the fabrication of high brightness (over 30,000 cd/m^2) top-emissive polymer light-emitting diodes (PLEDs) using a hybrid semi-transparent cathode, capable of the efficient injection of electrons. The composite cathode comprises the organic oxide/Al complex as the injection buffer layer covered by a thin Ag overlayer. The anode is made of Ag:Ag$_2$O coated on the glass substrate. The electroluminescence (EL) efficiency of 8.9 cd/A for phenyl-substituted poly(para-phenylene vinylene) copolymer based top-emissive PLED markedly exceeds that of 4.3 cd/A for the control device with the bottom-emissive configuration. The high performance is attributed to the balanced injection of charge carriers and the effective extraction of EL emission from the top cathode. The optical micro-cavity

---

[a] Author to whom all correspondence should be addressed; electronic mail: guotf@mail.ncku.edu.tw

effect significantly promotes the EL emission in the direction along the surface normal.

The top-emissive organic and polymer light-emitting diodes (T-OLEDs and T-PLEDs) emit light from the top surface of devices, which have many favorable features than the bottom-emissive O/PLEDs in active-matrix (AM) flat panel displays applications. [1-4] These diodes can be fabricated on opaque substrates, including rigid Si wafers and flexible steel foils. [5, 6] The complex driving circuits are placed under the O/PLEDs of the AM panels. The filling factor and the aperture ratio of a pixel are not constrained by the size of control units (transistor and capacitor). Therefore, top-emissive O/PLEDs can function at a lower bias voltage or current, while still exhibiting the same luminescence as bottom-emissive devices. The AM panels made of top-emissive O/PLEDs are expected to present a much more vividly colored image and the increased operating lifetime.

The configurations of typical T-O/PLEDs comprise several organic layers with different functionalities sandwiched between the highly reflective bottom anode and the semi-transparent top cathode. Ag is commonly adopted as a conductive bottom anode, because of its highest reflectivity of light in the visible region and its ability of the efficient injection for holes after the appropriate surface treatment. [7, 8] In the semi-transparent cathode, an ideal top electrode should be highly conductive of charges; support the efficient injection of electrons; be highly transparent to the light; have the high emission out-coupling efficiency, and have the long-term operating stability, etc. However, no single material satisfies all of the requirements of the top cathode simultaneously. Many research groups have applied an ultrathin layer of the low work function metals, LiF/Al, or the copper phthalocynaine covered with a thin Ag or the indium-tin-oxide (ITO) overlayer, to fabricate the top cathodes. [9-11, 3] The performance of T-O/PLEDs thus obtained was favorable. [12-16] A composite electrode is required to develop the multifunctional cathode structure. In

this manuscript, an organic oxide/Al/Ag composite cathode is reported for the fabrication of high-brightness and high-performance top-emissive PLEDs.

The configurations of the top-emissive PLEDs herein this study are plotted in the inset of Fig. 3. The Ag:Ag$_2$O electrode on the glass substrate, reported by Chen *et al.*, [7] is used as a highly reflective anode, and supports the efficient injection of holes in a top-emissive device. The thin layer of Ag$_2$O is prepared by UV-ozone treatment of the Ag/glass substrate. The device configuration comprises poly(3,4-ethylenedioxythiophene):polystyrenesulfonate (PEDOT:PSS Bayer Corp. 4083) as the hole transport layer, "high-yellow" phenyl-substituted poly(para-phenylene vinylene) copolymer (HY-PPV, EL emission centered at 560 nm) film as the light-emissive layer, and the hybrid organic oxide/Al/thin Ag as the semi-transparent cathode. The organic-oxide film is deposited by thermally evaporating a thin polymer layer, 15 Å, of poly(ethylene glycol) dimethyl ether (PEGDE) (Aldrich, Mn ca. 2,000) on the surface of HY-PPV film inside a vacuum chamber (10^{-6} torr). The semi-transparent metal electrode, 15 Å-thick Al layer and the Ag of the different thicknesses, is evaporated on the substrates sequentially without breaking the vacuum. No dielectric capping layer is utilized to the hybrid cathode in this study. For the bottom-emissive PLED, it comprises a transparent indium-tin-oxide (ITO)/glass substrate as the anode and the organic oxide/Al complex as the interface buffer layer covering with a thick(1200 Å), non-transparent layer of Ag as the device cathode. The active pixel area of the device is 0.06 cm^2. The details of the fabrication procedure and the current-brightness-voltage (*I-L-V*) measurement can be found elsewhere. [17, 18]

The usage of the organic oxide, PEGDE, as the cathode buffer layer enables the efficient

injection of electrons through the Al cathode and blocks the metal-induced quenching sites in the EL layer. [17, 18] Additionally, the enhanced performance is limited only to the use of Al metal. [18-20] The device configurations of the bottom-emissive devices with organic oxide/Al cathodes with Al metal layers of different thicknesses are glass/ITO/PEDOT:PSS/HY-PPV/PEGDE(15 Å)/Al(X Å)/Ag(1200 Å), with X= 5 Å, 15 Å, 50 Å, and 100 Å. Ag is used as the covering layer on the organic oxide/Al composite cathode to retain the conductivity of the electrode. The λ_{max} and the full width half maximum (FWHM) of the EL spectra are almost identical, λ_{max} at 560 nm and FWHM = 92 nm, for the bottom-emissive devices. However, the maximum efficiency is 10.7 cd/A at 6.70 V, 5142.0 cd/m^2 for the device with the PEGDE(15 Å)/Al(100 Å)/Ag(1200 Å) cathode (which has a thick Al middle layer), but only 3.4 cd/A at 6.20 V, 2831.9 cd/m^2 for the device with the PEGDE(15 Å)/Al(5 Å)/Ag(1200 Å) cathode structure (which has a thin Al middle layer). The luminous efficiencies are 9.1 cd/A at 6.70 V, 4824.8 cd/m^2 and 4.3 cd/A at 6.80 V, 5186.2 cd/m^2 for the devices with PEGDE(15 Å)/Al(50 Å)/Ag(1200 Å) and PEGDE(15 Å)/Al(15 Å)/Ag(1200 Å) cathode structure, respectively. The higher performance of the devices with thicker Al middle layers follows from the balanced injection of charge carriers, according to our previous investigations. [17, 18] A denser organic oxide/Al complex layer is expected to be generated at the interface of the composite cathode when the Al middle layer is thicker. Optimizing the thickness of the organic oxide/Al complex layer is critical to the injection of electrons through the cathode as well as the improvement in the performance of the device.

Figure 1 plots the *I-L-V* curves of the top- and the control bottom-emissive devices with the structures of glass/Ag:Ag$_2$O/PEDOT:PSS/HY-PPV/PEGDE(15 Å)/Al(15 Å)/Ag(70 Å) and glass/ITO/PEDOT:PSS/HY-PPV/PEGDE(15 Å)/Al(15 Å)/Ag(1200 Å), respectively. The

light intensity of the top-emissive device exceeds 30,000 cd/m^2 in the direction along the surface normal when biased at 8.80 V. The turn-on voltage of the light emission is under 3.0 V. Holes and electrons can be injected through the Ag:Ag$_2$O anode and the organic oxide/Al/Ag composite cathode, respectively, into the light-emitting polymer layer at the low bias. As shown in the inset in Fig. 1, the maximum luminous efficiency of the top-emissive device is 8.9 cd/A (6677.3 cd/m^2, EL emission centered at ~ 560 nm), when the device is biased at 6.60 V (74.98 mA/cm^2), in which the efficiency markedly exceeds that of 4.3 cd/A (5186.2 cd/m^2), biased at 6.80 V (120.40 mA/cm^2) for the control device with the bottom-emissive configuration. Since the cathode parts of the top- and control bottom-emissive devices comprise the same composition of the organic oxide/Al complex (PEGDE(15 Å)/Al(15 Å)) as the injection buffer layer for electrons, the superior luminous efficiency for the top-emissive device is presumed to be related to the enhanced spontaneous emission and the modified emission distribution of the optical micro-cavity effect. [21, 22, 12] The preferential direction of EL emission between the highly reflective Ag:Ag$_2$O anode and the semi-transparent organic oxide/Al/Ag cathode is tuned from the internal reflection toward the out-coupling regime. Hence, the device with the top-emissive configuration exhibits a substantially enhanced EL intensity in the forward direction, with a higher luminous efficiency along the direction of surface normal than that of the control bottom-emissive device without the cavity effect.

The internal reflections of the light that propagates between the highly reflective Ag:Ag$_2$O anode and the semi-transparent composite cathode are expected to have strong optical micro-cavity effects on both the spectral and the spatial distribution of the EL emission. [21-25] Figure 2 presents the normalized EL spectra of the control bottom-emissive device,

glass/ITO/PEDOT:PSS/HY-PPV/PEGDE(15 Å)/Al(15 Å)/Ag(1200 Å), and the top-emissive

devices made of Ag overlayers of various thicknesses,

glass/Ag:Ag$_2$O/PEDOT:PSS/HY-PPV/PEGDE(15 Å)/Al(15 Å)/Ag(Y Å), Y= 70 Å, 150 Å,

and 300 Å. The FWHM of the control bottom-emissive device is ~ 92 nm, but that of the

top-emissive device with the PEGDE(15 Å)/Al(15 Å)/Ag(70 Å) cathode structure is ~ 52 nm.

The shift in the λ_{max} toward the shorter wavelength (~ 560 nm to ~ 548 nm) and the decline in

the FWHM (~ 52 nm to ~ 24 nm) of the EL emissions were also observed for the top-emissive

devices with the thick and uniformly covering Ag overlayers. The redistribution of EL

emissions for top-emissive devices can therefore be attributed to optical micro-cavity effect.

The approximate calculation of the *Fabry-Perot* cavity theory is as follows, [21-23, 12]

$$G_{cav}(\lambda) = \frac{|E_{out}|^2}{|E_0|^2} \times \frac{\tau_{cav}}{\tau_{non-cav}}, \qquad S_{cav}(\lambda) = S_0(\lambda) \times G_{cav}(\lambda) \tag{1}$$

where $G_{cav}(\lambda)$ is the emission enhancement factor associated with the optical cavity at a single

wavelength λ. E_{out} and E_0 are the out-coupled and the free-space electric-field intensities of the

emissions, respecticely. τ_{cav} and $\tau_{non-cav}$ are the radiative lifetimes of the excited molecules in

the cavity and in free space, respectively. $S_0(\lambda)$ is the intrinsic emission spectrum of an emitter,

and is assumed to be a Gaussian. $S_{cav}(\lambda)$ represents the emission spectrum carrying under the

influence of the optical micro-cavity effect. The inset in Fig. 2 shows the simulated EL

emission, $S_{cav}(\lambda)$, determined by the calculation based on *Fabry-Perot* cavity theory and the

EL spectrum obtained in the direction along the surface normal of the top-emissive device

with the cathode structure, PEGDE(15 Å)/Al(15 Å)/Ag(300 Å). The simulated EL spectrum

overlaps substantially with the experimental result. The shift of λ_{max} from 560 nm (for the top-emissive device with a 70 Å-thick Ag covering layer) toward 548 nm (with a 300 Å-thick Ag covering layer), as observed in the Fig. 2, is probably caused by the change in the reflectivity of the composite cathode, which forms a complete cavity structure thus multiply reflects the EL emission and moves the λ_{max} toward the resonance wavelength of the optical cavity.

The simulation of FWHM is determined from Eq. (1) as follows, [23]

$$FWHM(\lambda) = \frac{\lambda^2}{2L}\left[\frac{1-\sqrt{R_1 R_2}}{\pi(R_1 R_2)^{1/4}}\right] \qquad (2)$$

where λ is the resonance wavelength, and L is the effective channel length in the cavity. R_1 and R_2 are the reflectivities of the anode (Ag:Ag$_2$O) and the composite cathode (organic oxide/Al/Ag), respectively. The reflectivity (R_2) is higher for the composite cathode with a thicker Ag overlayer. Therefore, the FWHM of the EL emissions is narrowed and the color of the top-emissive device is changed from the orange-yellow to a saturated green-yellow as the thickness of the Ag covering layer is increased.

Figure 3 illustrates the EL spectra of the top-emissive device, with the cathode structure PEGDE(15 Å)/Al(15 Å)/Ag(70 Å), measured at viewing angle of 0°, 30°, and 60° from the surface normal. The EL intensity is maximal in the forward direction of the substrate (0°), but decreases to 60 % and 45 % of the maximum intensity at the viewing angles of 30°, 60°, respectively. The net out-coupling efficiencies of the EL emissions (or the external quantum

efficiencies) for the top- and control bottom-emissive devices, as presented in Fig. 1, are compared by measuring the intensities of photocurrents through a photodiode inside an integrated sphere, which are approximately identical for both devices. Depositing an additional index matching layer onto the structure of the composite cathode is expected to increase the net EL out-coupling efficiency of the top-emissive devices. A theoretical simulation of the optical cavity structure and experimental work on the composite cathode with a supplementary light out-coupling layer are under way.

In summary, the organic oxide/Al/Ag composite electrode was disclosed as an appropriate cathode structure in the fabrication of the high-performance and high-brightness top-emissive PLEDs. The optical micro-cavity effect is responsible for the redistribution of EL emissions, in which the top-emissive devices exhibit saturated color emission and enhanced luminous intensity in the direction of the surface normal. The feasibility of applying an organic oxide/Al/Ag composite cathode in the small organic molecular T-OLED is also currently being conducted.

Reference

1. T. Sasaoka, M. Sekiya, A. Yumoto, J. Yamada, T. Hirano, Y. Iwase, T. Yamada, T. Ishibashi, T. Mori, M. Asano, S. Tamura, and T. Urabe, 2001 Society for Information Display (SID) International Symposium, Digest of Technical Papers, San Jose, CA, 2001, p. 384.

2. H. Riel, S. Karg, T. Beierlein, B. Ruhstaller, and W. Rieß, Appl. Phys. Lett. **82**, 466 (2003).

3. L. S. Hung, C. W. Tang, M. G. Mason, P. Raychaudhuri, and J. Madathil, Appl. Phys. Lett. **78**, 544 (2001).

4. M. –H. Lu, M. S. Weaver, T. X. Zhou, M. Rothman, R. C. Kwong, M. Hack, and J. J. Brown, Appl. Phys. Lett. **81**, 3921 (2002).

5. G. W. Jones, 2001 Society for information Display (SID) International Symposium, Digest of Technical Papers, San Jose, CA, 2001, p. 134.

6. Z. Xie, L. –S. Hung, and F. Zhu, Chem. Phys. Lett. **381**, 691 (2003).

7. C. –C. Chen, P. –Y. Hsieh, H. –H. Chiang, C. –L. Lin, H. –M. Wu, and C. –C. Wu, Appl. Phys. Lett. **83**, 5127 (2003).

8. Y. Q. Li, J. X. Tang, Z. Y. Xie, L. S. Hung, and S. S. Lau, Chem. Phys. Lett. **386**, 128 (2004).

9. G. Gu, V. Bulovic, P. E. Burrows, S. R. Forrest, and M. E. Thompson, Appl. Phys. Lett. **68**, 2606 (1996).

10. R. B. Pode, C. J. Lee, D. G. Moon, and J. I. Han, Appl. Phys. Lett. **84**, 4614 (2004).

11. L. S. Hung and C. W. Tang, Appl. Phys. Lett. **74**, 3209 (1999).

12. C. –L. Lin, H. –W. Lin, and C. –C. Wu, Appl. Phys. Lett. **87**, 021101 (2005).

13. L. Hou, F. Huang, W. Zeng, J. Peng, and Y. Cao, Appl. Phys. Lett. **87**, 153509 (2005).

14. S. –F. Hsu, C. –C. Lee, S. –W. Hwang, and C. H. Chen, Appl. Phys. Lett. **86**, 253508 (2005).

15. X. Y. Deng, M. K. Ho, and K. Y. Wong, J. Appl. Phys. **99**, 016103 (2006).

16. H. Peng, J. Sun, X. Zhu, X. Yu, M. Wong, and H. –S. Kwok, Appl. Phys. Lett. **88**, 073517 (2006).

17. T. –F. Guo, F. –S. Yang, Z. –J. Tsai, T. –C. Wen, S. –N. Hsieh, and Y. –S. Fu, Appl. Phys. Lett. **87**, 013504, (2005).

18. T. –F. Guo, F. –S. Yang, Z. –J. Tsai, T. –C. Wen, S. –N. Hsieh, Y. –S. Fu, and C, -T. Chung, Appl. Phys. Lett. **88**, 113501, (2006).

19. X. Y. Deng, W. M. Lau, K. Y. Wong, K. H. Low, H. F. Chow, and Y. Cao, Appl. Phys. Lett. **84**, 3522 (2004).

20. Y. –H. Niu, H. Ma, Q. Xu, and A. K. –Y. Jen, Appl. Phys. Lett. **86**, 083504 (2005).

21. A. Dodabalapur, L. J. Rothberg, R. H. Jordan, T. M. Miller, R. E. Slusher, and J. M. Philips, J. Appl. Phys. **80**, 6954 (1996).

22. R. H. Jordan, L. J. Rothberg, A. Dodabalapur, and R. E. Slusher, Appl. Phys. Lett. **69**, 1997 (1996).

23. E. F. Schubert, N. E. J. Hunt, M. Micovic, R. J. Malik, D. L. Sivco, A. Y. Cho, and G. J. Zydzik, Science **265**, 943 (1994).

24. N. Takada, T. Tsutsui, and S. Saito, Appl. Phys. Lett. **63**, 2032 (1993).

25. H. Becker, S. E. Burns, N. Tessler, and R. H. Friend, J. Appl. Phys. **81**, 2825 (1997).

Table I. The performance of top- and bottom-emissive PLEDs with hybrid organic oxide/Al/Ag cathodes.

Glass/ITO/PEDOT:PSS/HY-PPV/PEGDE (15 Å)/Al(**X** Å)/Ag(1200 Å)

Bottom-emissive PLEDs

	Maximum efficiency	λ_{max}	FWHM
Al(5 Å)	3.4 cd/A at 6.20 V, 81.98 mA/cm^2, 2831.9 cd/m^2	~ 560 nm	~ 92 nm
Al(15 Å)	4.3 cd/A at 6.80 V, 120.40 mA/cm^2, 5186.2 cd/m^2	~ 560 nm	~ 92 nm
Al(50 Å)	9.1 cd/A at 6.70 V, 53.03 mA/cm^2, 4824.8 cd/m^2	~ 560 nm	~ 92 nm
Al(100 Å)	10.7 cd/A at 6.70 V, 48.1 mA/cm^2, 5142.0 cd/m^2	~ 560 nm	~ 92 nm

Glass/Ag:Ag$_2$O/PEDOT:PSS/HY-PPV/PEGDE (15 Å)/Al(15 Å)/Ag(**Y** Å)

Top-emissive PLEDs

	Maximum efficiency	λ_{max}	FWHM
Ag(70 Å)	8.9 cd/A at 6.60V, 74.98 mA/cm^2, 6677.3 cd/m^2	~ 560 nm	~ 52 nm
Ag(150 Å)	4.9 cd/A at 5.80 V, 64.97 mA/cm^2, 3244.6 cd/m^2	~ 554 nm	~ 28 nm
Ag(300 Å)	1.0 cd/A at 5.90 V, 62.36 mA/cm^2, 646.0 cd/m^2	~ 548 nm	~ 24 nm

Figure Captions

FIG. 1.   *I-L-V* curves of (●) the top- and (○) the control bottom-emissive devices. The inset shows the plot of the luminous efficiency versus current density.

FIG. 2.   Normalized EL spectra of (○) the control bottom-emissive device, and the top-emissive devices made of Ag overlayers of various thicknesses, glass/Ag:Ag$_2$O/PEDOT:PSS/HY-PPV/PEGDE(15 Å)/Al(15 Å)/Ag(Y Å), Y= (●) 70 Å, (■) 150 Å, and (▲) 300 Å. The inset displays (△) the simulated EL emission and the (▲) measured EL spectrum of the top-emissive device with the cathode structure, PEGDE(15 Å)/Al(15 Å)/Ag(300 Å).

FIG. 3.   EL spectra of the top-emissive device, with the cathode structure PEGDE(15 Å)/Al(15 Å)/Ag(70 Å), measured at viewing angle of (●) 0°, (⊠) 30°, and (×) 60° from the surface normal. The inset shows the device configuration of the top-emissive PLEDs herein this study.
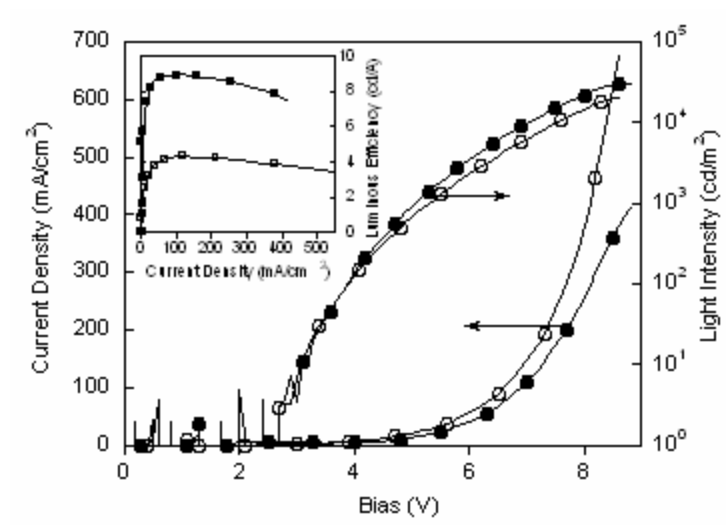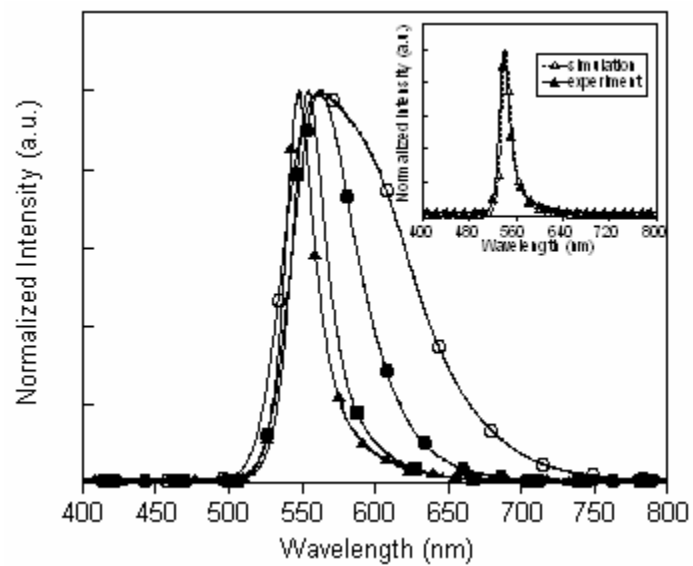
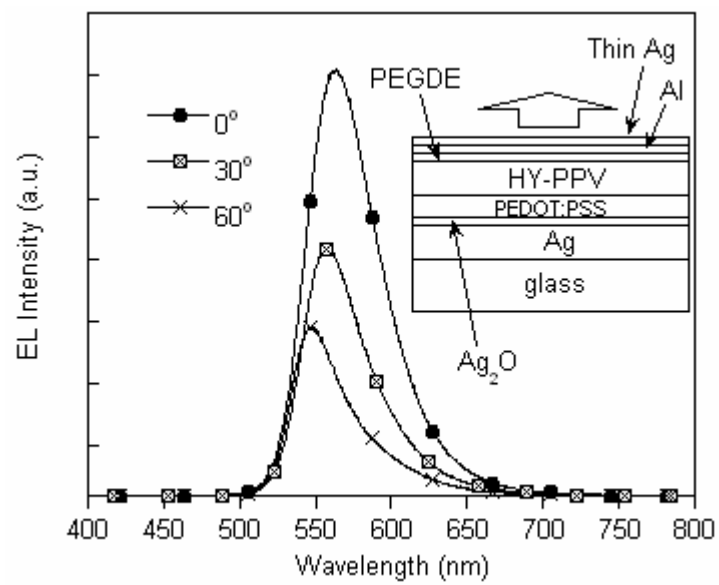Figure 1, Guo *et al.*

Figure 2, Guo *et al.*

Figure 3, Guo *et al.*

V. Organic oxide/Al composite cathode in organic/polymer light-emitting diodes

Tzung-Fang Guo,[a)] Fuh-Shun Yang, Zen-Jay Tsai

Institute of Electro- Optical Science and Engineering,

Advanced Optoelectronic Technology Center

National Cheng Kung University

Tainan, Taiwan 701, Republic of China

Ten-Chin Wen

Department of Chemical Engineering

National Cheng Kung University

Tainan, Taiwan 701, Republic of China

Ching-In Wu, Chia-Tin Chung

Chi Mei Optoelectronics Corporation

Tainan Science-Based Industrial Park

Taiwan, 741, Republic of China

Abstract

This study addresses the feasibility of using to fabricate the small molecular organic light-emitting diodes (OLEDs). A supplementary organic buffer film is placed at the interface between the tris-(8-hydroxyquinoline) aluminum (Alq$_3$) and the organic oxide/Al complex layers. Incorporating the rubrene/poly(ethylene glycol) dimethyl ether (PEGDE) buffer layers into the composite cathode structure markedly improves the performance of devices. The luminous efficiencies of Alq$_3$-based OLEDs biased at ~ 100 mA/cm^2 are 4.8 cd/A and 5.1 cd/A for rubrene(50 Å)/PEGDE(15 Å)/Al and rubrene(50 Å)/PEGDE(15 Å)/LiF(5 Å)/Al cathode devices, 1.3 cd/A and 3.8 cd/A for devices with Al and LiF(5 Å)/Al cathodes, respectively.

[a)] Author to whom all correspondence should be addressed; electronic mail: guotf@mail.ncku.edu.tw

Metals with low work functions, including calcium (Ca) and magnesium, or an ultrathin buffer layer of lithium fluoride (LiF) (<1 nm) at the interface of the electroluminescent film with the aluminum (Al) or the silver electrode, are now the frequently adopted cathode structures, effectively reducing the barrier to the injection of electrons at the cathode and greatly improving the performance of organic/polymer light-emitting diodes (O/PLEDs). [1-5] Recent studies had shown that blending the ionic surfactants in light-emitting polymer layers, or placing a thin layer of ionomers or organic salts which contain lithium (Li) or Ca ions on the surface of the electroluminescent films, with the high work function Al electrode yield the favorable cathode structures. The electroluminescence (EL) efficiencies of O/PLEDs exceed those of devices with conventional Ca/Al or LiF/Al cathodes. [6-9] However, our earlier works [10-11] and the most recent studies conducted by other groups [12-14] indicated that no salt ions need to be added to the cathode buffer layer. Simply casting an ultrathin layer (~ below 50 Å) of the polymers that have a sequent ethylene-oxide functional group, $(-CH_2CH_2O-)_n$, using a convenient spin-coating process [10, 14] or vacuum thermal deposition [11] can significantly increase the EL efficiencies of PLEDs. The devices with organic oxide/Al composite cathodes had a luminous efficiency that was approximately two orders of magnitude greater than that of devices with Al cathodes. The formation of an organic oxide/Al complex at the cathode interface, in which the complex layer supports the efficient injection of electrons through the Al cathode and blocks the mental-induced quenching sites in the EL (conjugated molecules) layer, is proposed. [10, 11]

The organic oxide/Al composite cathode is prepared by thermally evaporating the polymer with a low molecular weight, poly(ethylene glycol) dimethyl ether (PEGDE)

(Aldrich, Mn ~ 2,000), on the EL film under a vacuum. The Al metal electrode was then evaporated on the substrates without breaking the vacuum. [11] This approach can be easily integrated with the current manufacturing procedures to fabricate high-performance O/PLEDs. However, when the PEGDE/Al composite cathode was applied in the fabrication of small molecular OLEDs, the devices exhibited an almost Ohmic current-voltage (*I-V*) characteristic and very low electroluminescence. (The organic oxide/Al composite works very well with PLEDs.) Presumably, the electrical shorting of the device was caused by the interaction of the organic oxide/Al complex material with the tris-(8-hydroxyquinoline) aluminum (Alq$_3$) layer. The deposited Al metal punctured the Alq$_3$/ N,N′-bis-(1-naphthyl)-N,N′-diphenyl-1,1′-biphenyl-4-4′-diamine (NPB) layers and made contact with the indium-tin-oxide (ITO)/glass anode. The thicknesses of the Alq$_3$ or NPB layers is increased to prevent the flowing of any leakage current, but the *I-V* characteristic is not improved.

Although the reason for the electrical shorting of OLEDs of the organic oxide/Al composite cathodes is unclear, the problem can be solved by introducing an additional organic buffer layer into the configuration of the composite cathode. In this manuscript, a supplementary (50 Å-thick) organic buffer film, 5,6,11,12-tetraphenylnaphthacene (rubrene), is placed at the interface between the Alq$_3$ and PEGDE/Al complex layers. The luminescence efficiency of the Alq$_3$-based OLEDs is increased by a factor of ~ 4 from 1.3 cd/A to 4.8 cd/A when Al and rubrene(50 Å)/PEGDE(15 Å)/Al cathode are used.

The device configuration herein is comprised of ITO/glass substrate as the anode, NPB (500 Å) as the hole transport layer, Alq$_3$ (600 Å) as the light-emissive layer, an

organic supplementary film combined with an organic-oxide polymer as the interface buffer layers, and the Al metal cathode. Many organic small molecular materials, including rubrene, 1,3,5-tris(2-N-phenyl-benzimidzolyl)benzene (TPBI), pentacene, and 2,9-dimethyl-4,7-diphenyl-1,10-phenanthroline (BCP), were adopted as the supplementary layers in individual experiments and were thermally deposited on the Alq_3 layer under a high vacuum (10^{-6} torr). The active pixel area of the device was 0.06 cm^2. The current-brightness-voltage (*I-L-V*) measurements were made using a Keithley 2400 source measuring unit and a Keithley 2000 digital multimeter, with a silicon photodiode, calibrated using a Minolta LS-100 luminosity meter. All of the steps, except for a very short period of time (within 20 sec) to transport the substrates, were implemented inside a nitrogen-filled glove box. The photovoltaic measurement was performed under the illumination supplied by a Thermo Oriel 150W solar simulator (AM 1.5G).

Figure 1 plots the *I-L-V* curves of devices with an Al cathode, a thin Rubrene buffer layer (50 Å) with an Al cathode, and a thin rubrene buffer layer (50 Å) with a PEGDE(15 Å)/Al composite cathode. The OLED with the rubrene(50 Å)/ PEGDE(15 Å)/Al composite cathode exhibits the *I-V* characteristic of a diode. The injected current is much higher than that of a device in which Al is the cathode, at a given bias voltage. Additionally, the light turn-on voltage is brought forward to 4.5 V for the device with the rubrene(50 Å)/ PEGDE(15 Å)/Al cathode, which is 6.4 V for the device with the Al cathode. The higher injected current and the forward shift in the light turn-on voltage to the lower bias condition for the device with the rubrene(50 Å)/ PEGDE(15 Å)/Al cathode are attributable to the improvement in the electron injection through the Al electrode. The balance of injected charge carriers, holes and electrons, increases the electroluminescence and results

in the superior luminous efficiency of devices. As presented in the Fig. 2, the maximum luminous efficiency of the device with the composite cathode of the rubrene(50 Å)/PEGDE(15 Å)/Al is 5.1 cd/A (biased at 8.70V, 25.99 mA/cm^2, 1326.5 cd/m^2), while that of the Al cathode device is 1.3 cd/A (biased at 11.30V, 64.08 mA/cm^2, 827.0 cd/m^2). The luminous efficiency is also high for the device with the composite cathode biased at the high current and brightness regime. No variation in the EL emission, centered at 530 nm, between the Al and rubrene(50 Å)/PEGDE(15 Å)/Al cathode devices is observed as plot in the inset of Fig. 1. The device with the rubrene(50 Å)/Al cathode without a PEGDE buffer layer is considered for the comparison. Since the lowest unoccupied molecular orbital level of the rubrene is around 2.9 eV. [15] Incorporating a 50 Å-thick rubrene layer at the cathode interface interferes the injection of electrons through the Al cathode. Therefore, Fig. 1. clearly presents the lower injected current and the increase in the light turn-on voltage toward the higher bias condition, 9.7 V, of the rubrene/Al cathode device. The luminous efficiency is only 0.1 cd/A even lower than that of the Al cathode device. The decreased electron-injection barrier of organic oxide/Al composite cathode was fortified by the photovoltaic measurements. The inset in Fig. 2 presents the results of the photovoltaic measurements for devices with rubrene(50 Å)/Al and rubrene(50 Å)/PEGDE(15 Å)/Al cathodes. The higher open-circuit voltage (V_{oc}) of the device with rubrene/PEGDE/Al cathode suggests the higher built-in potential of the device. The rubrene/PEGDE/Al cathode has a lower work function as compared to that of the rubrene/Al cathode.

The luminous efficiency (under a bias of ∼ 100 mA/cm^2), the light turn-on voltage, and the λ_{max} of EL emissions of devices with the PEGDE(15 Å)/Al composite cathode with

rubrene buffer layers of the various thicknesses were studied and summarized in the upper portion of Table I. The luminous efficiency of the device with the rubrene(50 Å)/PEGDE(15 Å)/Al composite cathode is 4.8 cd/A (105.06 mA/cm^2); it is varied with the thicknesses of the rubrene buffer layers. The devices with 25 Å- and 100 Å-thick rubrene layers exhibit a red shift in the λ_{max} of EL emissions from ~530 nm to ~550 nm. A side peak from the rubrene(100Å)/PEGDE(15 Å)/Al cathode device at 590 nm is associated with the partial EL emission from the rubrene layer.

Figure 3 plots the *I-L-V* curves from the devices with PEGDE(15Å)/Al composite cathode with various organic buffer materials, TPBI, BCP, and pentacene. The inset in Fig. 3 presents the molecular structures. TPBI is often utilized as an effective electron injection and hole-blocking material for fabricating OLEDs. [16] However, the device with the TPBI(50 Å)/PEGDE(15 Å)/Al cathode has a lower injected current and a higher light turn-on voltage than the devices with the Al and rubrene(50 Å)/PEGDE(15 Å)/Al cathodes. When BCP (another organic material with high electron mobility and good hole-blocking capability) [17, 18] is used as the buffer layer in the composite cathode, the performance of the OLED is worse than that of the device in which only Al is used in the cathode. For the device with the 50 Å-thick pentacene buffer layer, the pentacene film did not work with the PEGDE(15 Å)/Al composite cathode in the same way as did the rubrene layer, although the molecular configuration of pentacene (which comprises the five continuously attached phenyl rings) is somehow analogous to the structure of the rubrene, as shown in the inset of Fig. 3. The light turn-on voltages are 7.4, 7.5, and 6.5 V and the luminous efficiencies of the TPBI(50 Å)/PEGDE(15 Å)/Al, the BCP(50 Å)/PEGDE(15 Å)/Al, and the pentacene(50 Å)/PEGDE(15 Å)/Al cathode devices are 2.8, 0.9, and 2.1 cd/A,

respectively, as listed in the Table I. The luminous efficiency of the TPBI(50 Å)/PEGDE(15 Å)/Al cathode device exceeds that of Al cathode device (1.3 cd/A), probably because of the confinement of excited excitons in the Alq_3 layer. TPBI is basically the organic material with high ionization potential.

The bottom part of Table I. summarized the performance of the control device with the LiF(5 Å)/Al cathode structure. The luminescence efficiency of the LiF(5 Å)/Al cathode device is increased by 35 % from 3.8 cd/A to 5.1 cd/A when rubrene(50 Å)/PEGDE(15 Å) buffer layers are added. The specific interaction of Al with ethylene oxide groups, $(-CH_2CH_2O-)_n$, during the deposition of the Al cathode is presumed to facilitate critically the injection of electrons through the Al cathode. The thin rubrene film and the organic oxide/Al complex layer together inhibit the electrical shorting of the devices. Hence, this combination represents a composite cathode structure that substantially improves the luminous efficiencies of OLEDs.

In summary, this study demonstrated the feasibility of using an organic oxide/Al composite cathode to fabricate small molecular OLEDs. The luminous efficiencies of Alq_3-based OLEDs are markedly increased by adding rubrene/PEGDE buffer layers to the composite cathode structure. The performance is enhanced by the balanced injection of charge carriers. The luminous efficiencies for rubrene(50 Å)/PEGDE(15 Å)/Al and rubrene(50 Å)/PEGDE(15 Å)/LiF(5 Å)/Al cathode devices at ~ 100 mA/cm^2 are 4.8 cd/A and 5.1 cd/A, and those of devices with Al and LiF(5 Å)/Al cathodes are 1.3 cd/A and 3.8 cd/A, respectively. The stability of the rubrene(50 Å)/PEGDE(15 Å)/Al device is tested by a constant current under a continuous bias, which is comparable to that of LiF/Al cathode

device. Studies of the interfacial reaction between the organic oxide/Al complex with Alq$_3$

and the rubrene buffer layers are currently underway.

Reference

26. D. Braun and A. J. Heeger, App. Phys. Lett. **58**, 1982 (1991).

27. C.W. Tang and S. A. VanSlyke, Appl. Phys. Lett. **51**, 913 (1987).

28. L. S. Huang, C. W. Tang, and M. G. Mason, Appl. Phys. Lett. **70**, 152 (1997).

29. G. E. Jabbour, Y. Kawabe, S. E. Shaheen, J. F. Wang, M. M. Morrell, B. Kippelen, and N. Peyghambarian, Appl. Phys. Lett. **71**, 1762 (1997).

30. J. Yoon, J. J. Kim, T. −W. Lee, and O. O. Park, Appl. Phys. Lett. **76**, 2152 (2000).

31. Y. Cao, G. Yu, and A. J. Heeger, Adv. Mater. **10**, 917 (1998).

32. J. Kido and T. Matsumoto, Appl. Phys. Lett. **73**, 2866 (1998).

33. T. −W. Lee, O. O. Park, L. −M. Do, T. Zyung, T. Ahn, and H. −K. Shim, J. Appl. Phys. **90**, 2128 (2001).

34. Q. Xu, J. Ouyang, Y. Yang, T. Ito, and J. Kido, Appl. Phys. Lett. **83**, 4695 (2003).

35. T. −F. Guo, F. −S. Yang, Z. −J. Tsai, T. −C. Wen, S. −N. Hsieh, and Y. −S. Fu, Appl. Phys. Lett. **87**, 013504, (2005).

36. T. −F. Guo, F. −S. Yang, Z. −J. Tsai, T. −C. Wen, S. −N. Hsieh, Y. −S. Fu, and C, -T. Chung, Appl. Phys. Lett. **88**, 113501, (2006).

37. J. H. Park, O. O. Park, J. −W. Yu, J. K. Kim, and Y. C. Kim, Appl. Phys. Lett. **84**, 1783 (2004).

38. X. Y. Deng, W. M. Lau, K. Y. Wong, K. H. Low, H. F. Chow, and Y. Cao, Appl. Phys. Lett. **84**, 3522 (2004).

39. Y. −H. Niu, H. Ma, Q. Xu, and A. K. −Y. Jen, Appl. Phys. Lett. **86**, 083504 (2005).

40. Z. −L. Zhang, X. −Y. Jiang, S. −H. Xu, T. Nagatomo, and O. Omoto, J. Phys. D **31**, 32 (1998).

41. Z. Gao, C. S. Lee, I. Bello, S. T. Lee, R. –M. Chen, T. –Y. Luh, J. Shi and C. W. Tang, Appl. Phys. Lett. **74**, 865 (1999).

42. Y. Kijima, N. Asai, and S. –I. Tamura, J. J. Appl. Phys. **38**, 5274 (1999).

43. D. F. O'Brien, M. A. Baldo, M. E. Thompson, and S. R. Forrest, Appl. Phys. Lett. **74**, 442 (1999).

Table I. The luminous efficiency, light turn-on voltage, and λ_{max} of EL emissions of devices with various cathode configurations.

Glass/ITO/NPB(500 Å)/Alq$_3$(600 Å)/**Organic buffer layer**/PEGDE(15 Å)/Al(1200 Å)

Organic buffer layer	Luminous efficiency	Light turn-on voltage	λ_{max}
Rubrene (25 Å)	0.3 cd/A at 7.40 V, 106.89 mA/cm^2, 306.0 cd/m^2	~ 4.3 V	~ 540 nm
Rubrene (50 Å)	4.8 cd/A at 9.50 V, 105.06 mA/cm^2, 5044.8 cd/m^2	~ 4.5 V	~ 530 nm
Rubrene (75 Å)	3.7 cd/A at 8.60 V, 96.73 mA/cm^2, 3618.4 cd/m^2	~ 4.3 V	~ 530 nm
Rubrene (100 Å)	2.7 cd/A at 9.60 V, 98.79 mA/cm^2, 2635.8 cd/m^2	~ 4.3 V	~ 550 nm & ~ 590 nm
TPBI (50 Å)	2.8 cd/A at 13.00 V, 103.77 mA/cm^2, 2963.9 cd/m^2	~ 7.4 V	~ 530 nm
BCP (50 Å)	0.9 cd/A at 13.30V, 105.61 mA/cm^2, 994.9 cd/m^2	~ 7.5 V	~ 530 nm
Pentacene (50 Å)	2.1 cd/A at 12.60 V, 105.70 mA/cm^2, 2254.7 cd/m^2	~ 6.5 V	~ 530 nm

Glass/ITO/NPB(500 Å)/Alq$_3$(600 Å)/ **Cathode**

Cathode	Luminous efficiency	Light turn-on voltage	λ_{max}
PEGDE (15 Å)/Al(1200 Å)	Ohmic	N/A	N/A
Al(1200 Å)	1.3 cd/A at 11.70 V, 108.01 mA/cm^2, 1382.1 cd/m^2	~ 6.4 V	~ 530 nm
Rubrene (50 Å)/Al(1200 Å)	0.1 cd/A at 14.40 V, 101.61 mA/cm^2, 100.8 cd/m^2	~ 9.7 V	~ 530 nm
LiF(5 Å)/Al(1200 Å)	3.8 cd/A at 8.50 V, 102.70 mA/cm^2, 3878.9 cd/m^2	~ 3.4 V	~ 530 nm
Rubrene (50 Å)/PEGDE (15 Å)/LiF(5 Å)/Al(1200 Å)	5.1 cd/A at 9.00 V, 104.26 mA/cm^2, 5297.1 cd/m^2	~ 3.6 V	~ 530 nm

Figure Captions

FIG. 1.   *I-L-V* curves of Alq$_3$-based devices with the ($\circ$) Al, ($\blacktriangledown$) rubrene(50 Å)/Al, and ($\bullet$) rubrene(50 Å)/PEGDE(15 Å)/Al cathodes. The inset plots the normalized EL spectra of the ($\circ$) Al and ($\bullet$) rubrene(50 Å)/PEGDE(15 Å)/Al cathode devices.

FIG. 2   The plot of the luminous efficiency versus current density of Alq$_3$-based devices with the ($\circ$) Al, ($\blacktriangledown$) rubrene(50 Å)/Al, and ($\bullet$) rubrene(50 Å)/PEGDE(15 Å)/Al cathodes. The inset shows the results of the photovoltaic measurement for devices with ($\blacktriangledown$) rubrene(50 Å)/Al and ($\bullet$) rubrene(50 Å)/PEGDE(15 Å)/Al cathodes.

FIG. 3.   *I-L-V* curves of Alq$_3$-based devices with ($\square$)TPBI(50 Å)/PEGDE(15Å)/Al, ($\blacktriangle$)BCP(50 Å)/ PEGDE(15Å)/Al, and ($\blacklozenge$)pentacene(50 Å)/ PEGDE(15Å)/Al composite cathodes. The inset shows the molecular structures of the rubrene, TPBI, pentacene, and BCP.
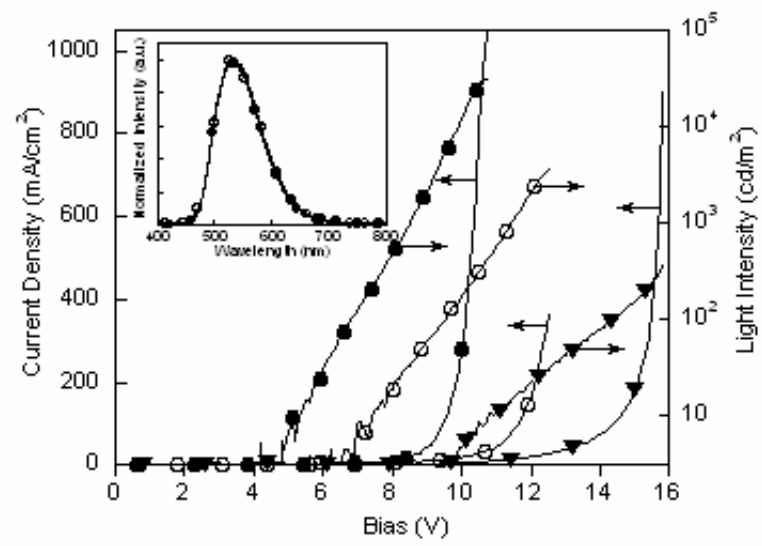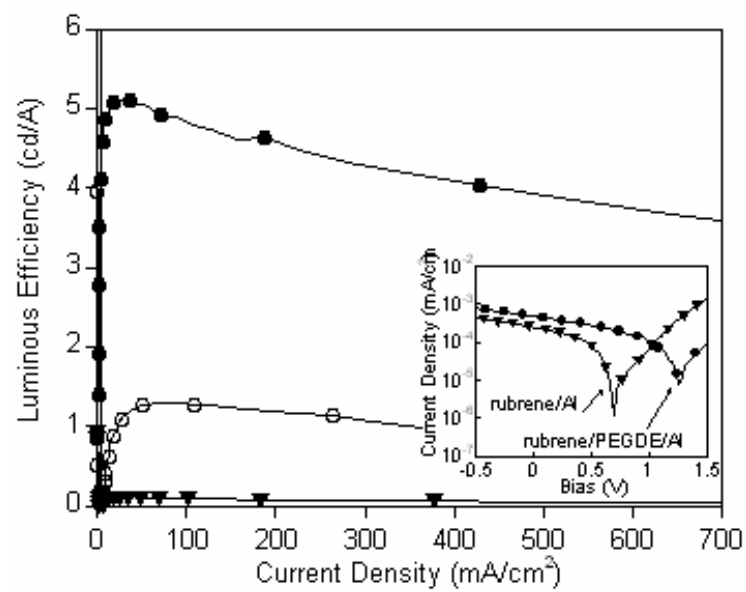
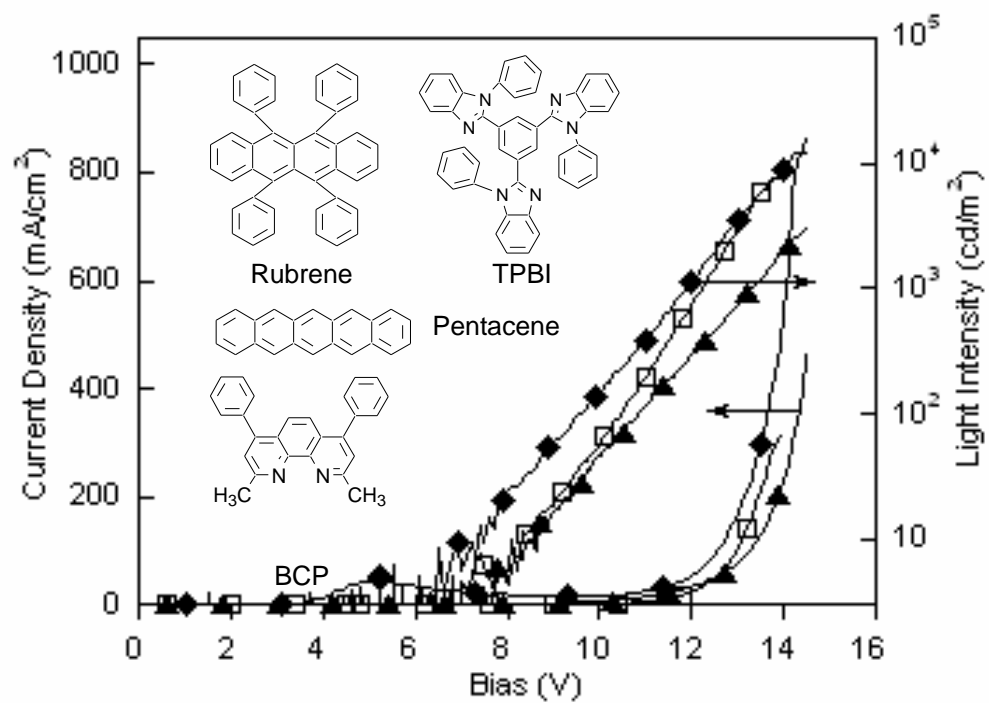Figure 1, Guo *et al.*

Figure 2, Guo *et al.*

Figure 3, Guo *et al.*

VI. Future work

- Extensive studies will be focused on the interfacial reaction between the organic-oxide nanolayer with Al, since it is important to the efficient injection of electron through the organic oxide/Al composite cathode into the light emissive layer.
- Depth-profile measurement of X-ray photoelectron spectroscopy will be used to *in-situ* characterize the unique carbon-metal properties at the cathode interface.
- Development of a novel Al-C nano-composite materials.

VII. Conclusions

The markedly enhanced device performance is presumed to be the instant formation of a specific carbon-Al complex nanolayer at the cathode interface during the deposition of Al. In 2007, we have proposed to proceed on the investigation of the unique organic-oxide nanolayer as the interfacial buffer structure for the fabrication of organic electronic devices. There are three major tasks under this research project, AOARD-07-4068, entitled "The organic-oxide interfacial layer on the studies of organic electronic devices (light-emitting diodes and solar cells)".

i) **Characterizations and the fundamental studies on the working mechanisms of the organic oxide ($-CH_2CH_2O-)_n$/Al composite nano-structure for organic electronic devices.**

ii) **The application of the organic oxide/Al composite electrode for high power conversion efficiency (PCE) polymer bulk-heterojunction (BHJ) solar cells.**

iii) **To set up a close team work with researcher and/or in the Universities funded by the Air Force of Scientific Research.**